Aerosol Reactor Theory: Stability and Dynamics of a Continuous Stirred Tank Aerosol Reactor

S. E. PRATSINIS
and S. K. FRIEDLANDER

Department of Chemical Engineering
University of California
Los Angeles, CA 90024

and

A. J. PEARLSTEIN

Aerospace and Mechanical
Engineering Department
University of Arizona
Tucson, AZ 85721

The stability characteristics of an aerosol reactor in a continuous stirred tank configuration have been investigated theoretically. Three dimensionless parameters, the surface tension group Σ, reaction rate group R, and residence time group θ_c, suffice to determine the dynamic behavior of this system. The stability of the unique steady state was investigated using linear analysis. Numerical integration of the full nonlinear equations shows that the dynamic behavior was in accord with the predictions of the linear stability theory. The system exhibits limit-cycle behavior in the unstable part of the parameter space. In the unstable region, a simple linear relation was found between the period of the numerically computed solutions and the bifurcation parameter, θ_c. The results of this study are in qualitative agreement with the experimental results of Badger and Dryden (1939).

SCOPE

Aerosol reactors are of interest in connection with the production of fine particles on a commercial scale. For a continuous reactor, stable, steady operation is necessary to insure constant aerosol product properties (e.g., particle size distribution). Indeed, sustained oscillations in particle number density and size distribution were reported by Badger and Dryden (1939) in their studies of "gum" particle formation in coal gas. The objective of the present paper was to investigate the stability characteristics of a simple type of aerosol reactor. The continuous stirred tank configuration was chosen because it is a well-established reactor type in industry. Stability criteria were sought in terms of the physical properties of the aerosol and the controllable operating variables of the reactor. Potential applications of this study are to controlled aerosol production in flow systems.

CONCLUSIONS AND SIGNIFICANCE

A theoretical study was conducted to investigate the stability characteristics of an aerosol reactor. In the model selected for study, aerosol particles are formed by homogeneous nucleation from molecules and molecular clusters of a single species that are produced by a zero-order chemical reaction. The particles grow by condensation and leave the system by the flow process.

Friedlander (1983) presented a set of four coupled nonlinear ordinary differential equations describing the aerosol dynamics in this system. Using this theoretical framework, the dynamic behavior of a continuous stirred tank aerosol reactor (CSTAR) was investigated by means of a linear stability analysis. It was found that three dimensionless groups suffice to determine the behavior of this system. These are: the surface tension group Σ, the reaction rate group R, and the residence time group θ_c.

For representative values of these parameters, the system was found to have a unique steady state. This was proved using interval analysis, a relatively new mathematical technique, and is consistent with the results of a nonrigorous graphical method.

By linearizing the system about the steady state, the conditions under which a small displacement from the steady state will grow were determined by examining the signs of the real parts of the temporal eigenvalues. The Routh-Hurwitz criterion was used to construct the surface separating the stable and unstable regions in the three-dimensional parameter space. In the stable region, a small perturbation from the steady state will die out after some transient period. In the unstable region, even the smallest perturbation will cause undamped oscillatory behavior in the system variables (such as aerosol number density, N).

This oscillatory performance can be explained as follows. Initially, monomer molecules are produced by chemical reaction in the CSTAR and aerosol particles are formed by homogeneous nucleation. New particle formation rapidly ceases because of monomer depletion by nucleation and condensation onto the aerosol surface. The monomer and aerosol particle concentrations are also depleted by outflow and wall losses. Monomer production continues by chemical reaction; when the number of particles

S. E. Pratsinis is currently at the Dept. of Chem. and Nuc. Eng., University of Cincinnati, Cincinnati, OH 45221-0171

(and consequently the available surface area for monomer condensation) drops below a certain value, homogeneous nucleation again becomes important and a new generation of particles is formed. In the unstable region of the parameter space, oscillations can be sustained indefinitely.

Choosing the dimensionless residence time θ_c as the bifurcation parameter, it was found that a simple Hopf bifurcation (two complex conjugate eigenvalues crossing into the right halfplane) occurs as θ_c increases. In the unstable region, a simple linear relationship exists between the oscillation period and θ_c. It was found that by increasing θ_c, the two complex conjugate eigenvalues do not move further into the real positive plane, but at a certain value of θ_c they "return" and slowly approach the origin of the complex plane. The response diagrams provide a quantitative description of the effect of instability on the dependent variables of the system. The present analysis qualitatively explains the results obtained by Badger and Dryden (1939) in their study of particle formation in coal gas. The lack of information concerning the properties of the condensing aerosol and the reaction rate in their system prevents quantitative comparisons between the two studies.

INTRODUCTION

Aerosol reactors have been used to investigate the behavior of aerosols in laboratory studies (smog studies), as well as for the production of fine particles in industry and in laboratory research. Friedlander (1982) outlined the basic types of aerosol reactors according to their operational characteristics. He also pointed out the need to develop rigorous theoretical models applicable to the design of industrial aerosol reactors. The purpose of this paper is to investigate the stability characteristics of aerosol reactors.

Periodic phenomena have previously been observed in aerosol systems of industrial interest. Badger and Dryden (1939) were the first investigators to report oscillatory behavior in the aerosol number density and particle size. They studied aerosol formation by chemical reaction between certain diolefins (cyclopentadiene and butadiene) and trace amounts of NO in coal gas effluents. The reaction chamber in their studies was a holding tank where the reactant gases were held for a specified time and the aerosol concentration and particle size were measured by means of an ultramicroscope and an optical microscope. At certain values of the controllable parameters of their system, they observed sustained oscillations of the aerosol number density as a function of time throughout the duration of their experiments. Badger and Dryden reported that the period of oscillation depended on the residence time in the holding tank and the amount of NO in the inlet stream.

Periodic phenomena have also been observed in other particle forming systems. Reiss et al. (1977) observed oscillatory behavior of the nucleation rate in a diffusion cloud chamber during the photooxidation of SO_2. Heist et al. (1980) also observed oscillations in the number of methanol droplets in diffusion cloud chamber studies of the homogeneous nucleation of methanol. One should note, however, that the formation of aerosol in diffusion cloud chambers is driven by mass transport, while aerosol formation in aerosol reactors is driven by the rate of chemical reaction. A continuous industrial crystallizer is somewhat similar to the continuous stirred tank aerosol reactor (CSTAR), since nucleation and particle growth are important in both systems. Time-periodic phenomena have been observed in crystallizers, and linear stability analysis has been extensively used to predict the regions of the parameter space in which oscillatory behavior in crystal size distribution and number density will occur (Sherwin et al., 1967; Randolph, 1980; Jerauld et al., 1983).

Friedlander (1977) outlined the principles of aerosol reactors operating in the CSTR mode and gave simple analytical solutions for the aerosol size distribution for some limiting cases. Crump and Seinfeld (1980) developed a theoretical model of aerosol behavior in a continuous stirred tank reactor. For an arbitrary inlet aerosol size distribution and for a coagulation coefficient and particle growth rate independent of particle size, they obtained exact solutions for the steady state aerosol distribution. Friedlander (1983) presented a theoretical model for aerosol formation by chemical reaction in the absence of coagulation in batch and flow aerosol reactors. His analysis resulted in four coupled nonlinear ordinary differential equations that determined the dynamic behavior of the aerosol. He also described a method that can be used to investigate the stability characteristics of an aerosol flow reactor.

In this paper, a theoretical study of the stability characteristics of a CSTAR is presented using Friedlander's (1983) model. The CSTAR configuration was chosen because it is a relatively simple system to model. In addition, experiments showing the existence of oscillatory phenomena in these systems have been carried out in a similar reactor configuration (Badger and Dryden, 1939). Using linear stability analysis, the stability criteria are expressed in terms of dimensionless groups of parameters, which are simple functions of the physical properties of the aerosol and the controllable operating variables of the reactor. Since the stability criteria can be presented in terms of parameters that are independent of the steady state values of the dependent variables, the results of the study can be easily interpreted in terms of design parameters in order to test the theory.

MODEL DESCRIPTION

The model to be considered here has been discussed by Friedlander (1983), so we will confine our remarks to a brief description of the overall process.

The CSTAR is a well mixed, isothermal, constant volume tank into which the reactant gases are carried at a constant flow rate. Inside, they react and form a single, condensable (low vapor pressure) molecular species by a zero-order chemical reaction with rate $\tilde{R}$. Molecular collisions between the condensable molecules (monomers) produce stable aerosol particles consisting of k^* (critical size) molecules at a rate, $\tilde{I}$, according to classical nucleation theory. The newly formed particles grow according to the molecular bombardment growth mechanism by scavenging molecules (monomers) onto their surfaces of total are $\tilde{A}$, until they leave the system in the product stream. Monomer, cluster, and particle wall losses, coagulation, subcritical cluster scavenging, and the effect of particle surface curvature on aerosol evaporation rate (Kelvin effect) are neglected.

Thus, one can write a mass balance for the monomer concentration:

$$\frac{dn_1}{dt} = \tilde{R} - \tilde{I}k^* - (n_1 - n_s)\left(\frac{k_B T}{2\pi m_1}\right)^{1/2}\tilde{A} - \frac{n_1}{\tau} \qquad (1)$$

where n_s is the monomer concentration at saturation conditions,

m_1 is the monomer mass, and τ is the residence time of the CSTAR. The first term on the righthand side of Eq. 1 represents the rate of introduction of new monomers into the system. The second term represents the rate at which monomers are consumed in the formation of new aerosol by nucleation. The third term stands for the net rate at which monomers are lost by condensation and gained by evaporation from the surface of the aerosol. The last term accounts for the monomer lost from the system by outflow.

The rate of change of the various moments of the aerosol size distribution in this system can be written in the same way (Friedlander, 1983):

Aerosol surface area, $\tilde{A}$

$$\frac{d\tilde{A}}{dt} = \tilde{I}k^{*2/3}s_1 + 2\pi B_1(S-1)\tilde{M}_1 - \frac{\tilde{A}}{\tau} \tag{2}$$

First moment, $\tilde{M}_1$

$$\frac{d\tilde{M}_1}{dt} = \tilde{I}k^{*1/3}d_1 + (S-1)B_1\tilde{N} - \frac{\tilde{M}_1}{\tau} \tag{3}$$

Aerosol number density, $\tilde{N}$

$$\frac{d\tilde{N}}{dt} = \tilde{I} - \frac{\tilde{N}}{\tau} \tag{4}$$

where

$$B_1 = 2n_s v_1 \left(\frac{k_B T}{2\pi m_1}\right)^{1/2}$$

$$S = \frac{n_1}{n_s} \qquad \text{saturation ratio}$$

and d_1, s_1, v_1 are the monomer diameter, surface area, and volume, respectively. The nucleation rate is given by the classical theory of homogeneous nucleation (Frenkel, 1955) as:

$$\tilde{I} = n_s^2 s_1 \left(\frac{k_B T}{2\pi m_1}\right)^{1/2} \left(\frac{1}{6\pi}\right)^{1/3} k^{*1/6} (\ln S)^{1/2} S^{2-k^*/2} \tag{5}$$

and the critical particle size, k^*, is given by

$$k^* = \frac{32\pi}{3(\ln S)^3}\left(\frac{\sigma v_1^{2/3}}{k_B T}\right)^3 \tag{6}$$

Introducing the set of dimensionless variables and parameters shown in Table 1, the system of Eqs. 1–6 can be rewritten in dimensionless form as

$$\frac{dS}{d\theta} = R - Ik^* - (S-1)A - \frac{S}{\theta_c} \tag{7}$$

$$\frac{dA}{d\theta} = Ik^{*2/3} + \frac{2}{3}(S-1)M_1 - \frac{A}{\theta_c} \tag{8}$$

$$\frac{dM_1}{d\theta} = Ik^{*1/3} + \frac{1}{3}(S-1)N - \frac{M_1}{\theta_c} \tag{9}$$

$$\frac{dN}{d\theta} = I - \frac{N}{\theta_c} \tag{10}$$

$$I = \left(\frac{2}{9\pi}\right)^{1/3} \Sigma^{1/2} S^{2-k^*/2} \tag{11}$$

$$k^* = \frac{\pi}{6}\left(\frac{4\Sigma}{\ln S}\right)^3 \tag{12}$$

Thus, given the dimensionless parameters Σ, R, and θ_c, and the initial values of S, A, M_1, and N, one can calculate the aerosol properties as functions of time without computing the size distribution of the aerosol.

TABLE 1. DIMENSIONLESS VARIABLES AND PARAMETERS

Group	Physical Meaning
$S = \frac{n_1}{n_s}$	Saturation ratio
$\Sigma = \frac{\sigma v_1^{2/3}}{k_B T}$	Surface tension
$I = \frac{\tilde{I}}{n_s^2 s_1 (k_B T/2\pi m_1)^{1/2}}$	Nucleation rate
$R = \frac{\tilde{R}}{n_s^2 s_1 (k_B T/2\pi m_1)^{1/2}}$	Reaction rate
$N = \frac{\tilde{N}}{n_s}$	Number density
$M_1 = \frac{\tilde{M}_1}{n_s d_1}$	First moment
$A = \frac{\tilde{A}}{n_s s_1}$	Aerosol area
$\theta = n_s s_1 (k_B T/2\pi m_1)^{1/2} t$	Time
$\theta_c = n_s s_1 (k_B T/2\pi m_1)^{1/2} \tau$	Residence time

CALCULATION OF THE STEADY STATE

By setting the lefthand sides of Eqs. 7–10 equal to zero, the steady state equations

$$N_o = I_o \theta_c \tag{13}$$

$$M_{1o} = \left[I_o k_o^{*1/3} + \frac{1}{3}(S_o - 1)N_o\right]\theta_c \tag{14}$$

$$A_o = \left[I_o k_o^{*2/3} + \frac{2}{3}(S_o - 1)M_{1o}\right]\theta_c \tag{15}$$

$$S_o = \left[R - I_o k_o^* - (S_o - 1)A_o\right]\theta_c \tag{16}$$

are obtained, where I_o and k_o^* are the functions I and k^* evaluated at $S = S_o$. By successive substitution of Eqs. 13, 14, and 15 into Eq. 16, the following expression is obtained

$$f(S_o) = R - \frac{S_o}{\theta_c} - I_o k_o^* - (S_o - 1)\theta_c \left\{ I_o k_o^{*2/3} + \frac{2}{3}(S_o - 1)\theta_c \left[I_o k_o^{*1/3} + \frac{1}{3}(S_o - 1)\theta_c I_o \right] \right\} = 0 \tag{17}$$

Substituting Eqs. 11 and 12 into Eq. 17 results in a transcendental equation involving the single variable S_o. The zeros of this equation can be found using Muller's algorithm as implemented in the standard subroutine ZREAL1 (IMSL, 1980).

At this point, the question arises as to how many steady states are possible in this system. In Figure 1, one can see the dependence of the steady state saturation ratio, S_o, on R for various values of θ_c and a fixed value of Σ. The numerical results indicate that R is a monotonic function of S_o, and that dR/dS_o is positive for the values of the system parameters shown. This provides strong evidence that the system has a unique steady state, but it is not a rigorous proof of the uniqueness of the solution $S_o(R; \theta_c, \Sigma)$. If it

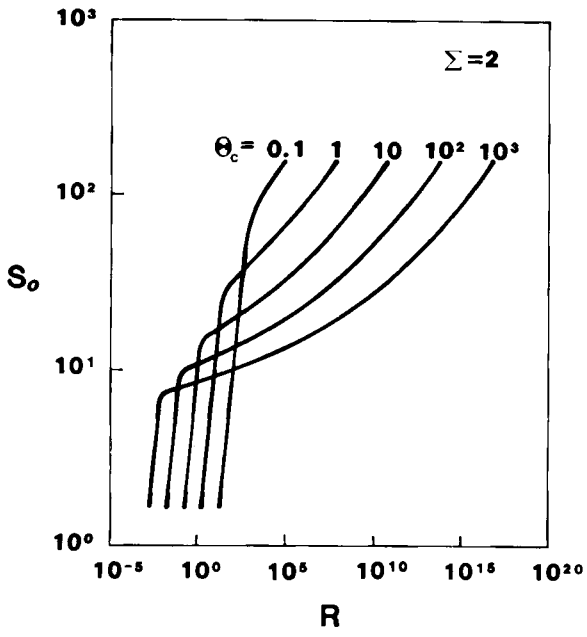

Figure 1. Schematic plots of Eq. 17 showing uniqueness of steady state. In all cases R is a monotonic function of S_o and dR/dS_o is positive.

can be shown that $dR/dS_o > 0$ always, then the conclusion would be rigorous (Uppal et al., 1974; Jerauld et al., 1983).

In this problem, uniqueness can be rigorously established by the use of interval analysis (Moore, 1979), combined with a contraction mapping based on either the Schauder or Brouwer fixed point theorems (Moore and Jones, 1977). Given the values of the parameters Σ, R, and θ_c, we can establish the uniqueness or nonexistence of a zero S_o of the function f in Eq. 17, in the finite interval $[S_o] = [\underline{S}_o, \bar{S}_o]$. This technique is extendable to n equations in n unknowns, and is useful in a variety of engineering problems, because the range of the variables is often known and finite. (For example, in CSTR problems the reactant conversion varies from zero to unity; in our case, the saturation ratio may vary from unity up to some finite value determined by the initial conditions.) In our work, we use the algorithm of Krawczyk (1969), as extended by Moore and Jones (1977). Here, an interval $[S_o^{(v)}]$ thought to contain a zero of f is mapped into a new (possibly smaller) interval $[S_o^{(v+1)}]$ by the scheme

$$[S_o^{(v+1)}] = [S_o^{(v)}] \cap [K([S_o^{(v)}])] \tag{18}$$

$$\left[K([S_o^{(v)}])\right] = \left[y^{(v)} - Y^{(v)} f(y^{(v)}) + \left(1 - Y^{(v)}\left[\frac{df([S_o^{(v)}])}{dS_o}\right]\right)([S_o^{(v)}] - y^{(v)})\right], \tag{19}$$

$y^{(v)}$ is the midpoint of the interval $[S_o^{(v)}]$, $Y^{(v)}$ is the inverse of the midpoint of the interval $[df([S_o^{(v)}])/dS_o]$, and the square brackets denote an interval. With the exception of the calculation of the upper and lower bounds of the interval $[df([S_o^{(v)}])/dS_o]$, the interval arithmetic operations in Eq. 19 are easily performed (Moore, 1979).

If the interval $[S_o^{(v+1)}]$ formed in Eq. 18 is empty, then $[S_o^{(v)}]$ does not contain a zero of f. If $[S_o^{(v+1)}]$, is strictly included in $[S_o^{(v)}]$, then f has at least one zero in $[S_o^{(v)}]$, the uniqueness of which can be decided according to the method described in theorem 5.4 of Moore (1979). If neither of these situations obtains, $[S_o^{(v+1)}]$ is bisected and the algorithm, Eqs. 18–19, is repeated until either uniqueness or nonexistence is established, or the bisected intervals are too small for the available machine precision. This last possibility did not arise in the present work.

This method was successfully applied in our case and convergence to the unique steady state was always achieved. However, it should be noted that special care was required in bounding df/dS_o on $[S_o^{(v)}]$.

STABILITY ANALYSIS

To determine the conditions under which a CSTAR exhibits stable or unstable behavior, a linear stability analysis was performed. Equations 7–10 were linearized about the steady state, and conditions for the growth of a small perturbation about the steady state were determined using the Routh-Hurwitz criteria. Denoting the disturbances to the steady state by S', A', M'_1, and N', the linear perturbation equations are

$$\frac{dS'}{d\theta} = \left[-\left(\frac{dIk^*}{dS}\right)_o - A_o - \frac{1}{\theta_c}\right] S' - (S_o - 1)A'$$

$$\frac{dA'}{d\theta} = \left[\left(\frac{dIk^{*2/3}}{dS}\right)_o + \frac{2}{3} M_{1o}\right] S' - \frac{1}{\theta_c} A' + \frac{2}{3}(S_o - 1)M_1'$$

$$\frac{dM_1'}{d\theta} = \left[\left(\frac{dIk^{*1/3}}{dS}\right)_o + \frac{1}{3} N_o\right] S' - \frac{1}{\theta_c} M_1' + \frac{1}{3}(S_o - 1)N'$$

$$\frac{dN'}{d\theta} = \left(\frac{dI}{dS}\right)_o S' - \frac{1}{\theta_c} N'.$$

For $b = 0, 1/3, 2/3, 1$ it can be easily shown that

$$\left(\frac{dIk^{*b}}{dS}\right)_o = \frac{I_o k_o^{*b}}{S_o}\left(k_o^* + 2 - \frac{3b}{\ln S_o}\right).$$

The characteristic equation of this system is an algebraic equation of the form $\lambda^4 + \alpha\lambda^3 + \beta\lambda^2 + \gamma\lambda + \delta = 0$ where α, β, γ, and δ are highly nonlinear functions of the dimensionless parameters and the steady state values of the dependent variables (Appendix). Simultaneous satisfaction of the conditions:

$$\alpha,\beta,\gamma,\delta > 0$$
$$\gamma^2 - \alpha\beta\gamma + \alpha^2\delta < 0 \tag{20}$$

(Karman and Biot, 1940) is necessary and sufficient for the stability of the steady solution of Eqs. 7–10. As one can see in the Appendix, the coefficients of the characteristic equation are always positive. Hence $\gamma^2 - \alpha\beta\gamma + \alpha^2\delta = 0$ becomes the criterion that can be used to construct the surface separating the stable and unstable regions in the three-dimensional parameter space. The dependence of the criterion on the steady state variables is implicitly eliminated using Eqs. 13–17. Figure 2 shows the location of three different stability boundaries for four values of Σ, in the $R - \theta_c$ plane. For $d_p > d_p^*$, the Kelvin effect was neglected in Eqs. 1–3. The validity of this assumption was tested in a separate analysis by substituting $(S - S^{d_p^*/d_p}$ for $(S - 1)$ in Eqs. 1–3. For $\Sigma > 1.8$, the location of the stability boundary was not affected by neglecting the Kelvin effect.

For a given aerosol species, Σ is a fixed parameter that is calculated from the physical properties of the substance. For example, $\Sigma = 2.4$ for ethane sulfinic acid at 20°C as estimated by Becker and Reiss (1976); $\Sigma = 2.9$ for NH_4Cl at 23°C (Henry et al.,

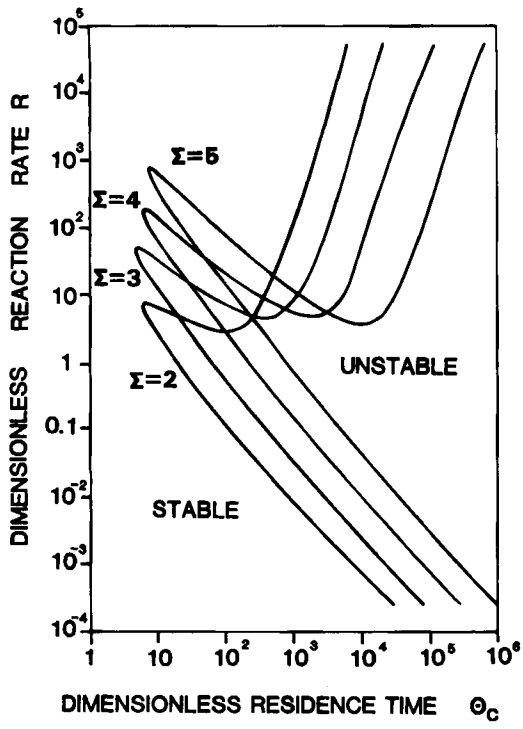

Figure 2. Stability map in the $R - \theta_c$ plane. Each curve, corresponding to a fixed value of Σ, separates the stable (left) from the unstable (right) parts of the parameter space.

1983); and $\Sigma = 4.7$ for dibutylphthalate and $\Sigma = 5.2$ for aluminum sec-butoxide at 25°C. Generally, Σ decreases with increasing temperature. In the experiments of Henry et al. (1983) Σ was decreased from 4.7 to 2.1 by increasing T from 253 to 296 K. The value of R can be controlled by varying the concentrations of the reactants or, for a photochemical system, by varying the intensity of the light source. In production of NH_4Cl aerosol, R varied from 10^{-2} to 10^3 for various combinations of NH_3 and HCl concentrations. The easiest parameter to control is θ_c, which can be varied by adjusting the flow rate of the reactant gases or the size of the reaction vessel ($\theta_c = 1{,}000$ corresponds to $\tau = 27$ s in a CSTAR producing NH_4Cl aerosol at 300 K, or to $\tau = 35$ min in a CSTAR producing dioctylphthalate aerosol).

Since θ_c is the most convenient parameter to control in our system, one can examine the stability of the aerosol reactor by using θ_c as the bifurcation parameter of the system. Thus, for fixed Σ and R, one can change the behavior of the system from stable to unstable by increasing θ_c. The existence of a unique but unstable steady solution in this system guarantees the existence of at least one (attracting) solution which does not asymptotically approach a steady state. In our case, we have a Hopf bifurcation since two complex conjugate eigenvalues cross the imaginary axis at the bifurcation point while the other two remain real and negative. Thus, there will be a limit-cycle solution when the system operates in the unstable region of the parameter space. This limit cycle may itself be stable or unstable (Marsden and McCracken, 1976, pp. 91 et seq.).

The location of the complex conjugate pair of eigenvalues in the unstable right half-plane (RHP) was investigated as a function of the bifurcation parameter, θ_c, and the rather interesting behavior shown in Figure 3a was observed. Fixing $\Sigma = 2$ and $R = 100$, θ_c was varied from 100 to 10,000, while the bifurcation point was found to be at $\theta_{c,BP} = 829$. By increasing θ_c, the complex conjugate eigenvalue pair crosses the imaginary axis and moves further into the RHP. However, at a certain value of θ_c (in this case $\theta_c = 2{,}000$), the pair of complex eigenvalues starts to "return" toward the imaginary axis and asymptotically approaches the origin of the complex plane from the RHP. At the same time, one of the two real negative eigenvalues (not shown in Figure 3a) asymptotically approaches the origin of the complex plane from the left side, while the fourth eigenvalue approaches minus infinity. Aris (1975) has reported the results of Lee (1970) in this form, showing the effect of the Lewis number on the stability of an exothermic reaction occurring inside a porous catalyst pellet. The present results show that as the system "moves" further into the unstable region, the system becomes "less unstable." To our knowledge this is the first time that such an eigenvalue movement in the RHP has been reported. We investigated the real part of the unstable eigenvalues in the RHP by using a modified form of the Routh-Hurwitz criterion. In Figure 3b are shown the isopleths of the real part, λ_r, of the most unstable eigenvalues of the linear perturbation equations. It is clearly seen that the largest values of λ_r are confined to a relatively small region of the parameter space, close to the stability boundary. This result may be of some engineering significance, such as in the design of controls for a CSTAR.

RESULTS

To provide evidence for the stability of the limit cycle solutions, the dynamic response of the full nonlinear system, Eqs. 7–10, was examined for two sets of parameter values located in the stable and unstable parts of the parameter space. Thus, in Figures 4a and b, the response of the system in the stable region is shown for $\Sigma = 2$, $R = 100$, and $\theta_c = 30$. The aerosol number density has been plotted as function of time (Figure 4a). Here, time has been expressed as a multiple of the reactor's residence time, which is a more convenient variable for a CSTAR. It is seen that a perturbation in N dies out after some transient period. In Figure 4b, a two-

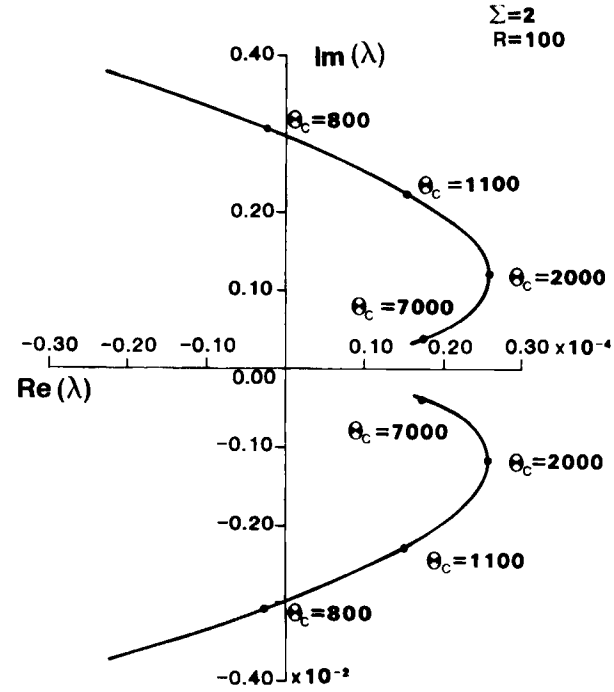

Figure 3a. Movement of unstable eigenvalues of the linearized system as a function of bifurcation parameter θ_c in the complex plane.

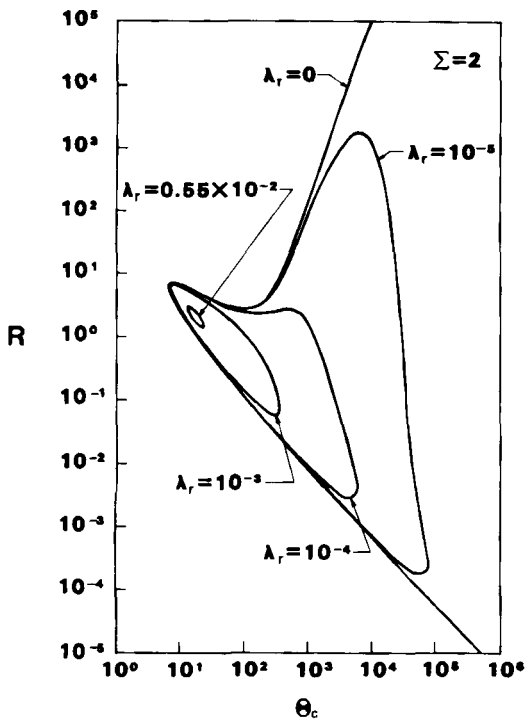

Figure 3b. Isopleths of positive real parts of unstable eigenvalues in the unstable region. Isopleth $\lambda_r = 0$ corresponds to the marginal stability boundary.

dimensional projection of a typical phase space trajectory, corresponding to the approach to a stable steady state, is shown. In Figures 5a and b, the dynamic response of the system is examined for $\Sigma = 2$, $R = 100$, $\theta_c = 3{,}000$, for which the linear analysis indicates that the steady state is unstable and the Hopf theorem (Marsden and McCracken, 1976) implies the existence of a limit cycle. In this case, N oscillates around its unstable steady value (Figure 5a) and an apparently stable limit cycle appears to surround the steady solution in this two-dimensional projection (Figure 5b). The behavior of the nonlinear system was examined for various values of the system parameters and in all cases was found to be consistent with the predictions of the linear theory. This indicates that the boundaries mapped out by the linearized stability analysis actually separate stable and unstable behavior of the nonlinear system.

From Figure 5a, one can estimate the oscillation period. It is of interest to find the dependence of the period on the system parameters, since our system exhibits a typical Hopf bifurcation. According to Hopf's theorem (Marsden and McCracken, 1976) the period of the limit cycle at the bifurcation point is given by $T_{BP} = 2\pi/|\lambda_{im}|$ where the denominator is the absolute value of the imaginary eigenvalues at the bifurcation point. In principle, this formula is valid only on the stability boundary, and nowhere else in the parameter space. The question frequently arises (e.g., Jerauld et al., 1983) as to the validity of this expression as one moves away from the bifurcation point. Jerauld et al. modeled crystal formation and growth in a continuous crystallizer and found that the period of oscillation at the stability boundary was a good estimate of the period of oscillation "far away" from the stability boundary in the unstable part of the parameter space. The possibility of a similar result in our system was quantitatively investigated. In Figure 6, the ratio of the period T_N of the numerical solution of Eqs. 7–10 to the period T_{BP} at the bifurcation point is plotted against the bifurcation parameter, θ_c, for fixed Σ and R. For $\Sigma = 2$ and $R = 100$ the bifurcation point is at $\theta_{c,BP} = 829$ where the period ratio is unity by definition. In the range of θ_c values from 829 to 10^5 a simple linear relationship was found to hold between the period ratio and the bifurcation parameter. Thus, one can write

$$T_N = T_{BP}\left(\frac{\theta_c}{\theta_{c,BP}}\right)^h \tag{21}$$

for the oscillation period in the unstable region (where $h = 1$ in this case). Therefore, the use of T_{BP} as the period in the unstable parameter region is not valid. The magnitude of the error for such an assumption will be a function of the "distance" from the bifurcation point and can be calculated from Eq. 21.

From an engineering point of view, it is of interest to know the amplitude of oscillation of the system variables (e.g., N) as a function of the bifurcation parameter (e.g., θ_c). The standard way to show this dependence is by constructing a response diagram, as shown in Figure 7 for N as a function of θ_c for $R = 100$ and $\Sigma = 2$. The solid line shows the steady response of N as a function of θ_c in the stable region. The heavy black dot indicates the value of N at the bifurcation point. The dashed line shows the unstable steady state values of N bounded above and below by an envelope of points showing the minimum and maximum values of N dur-

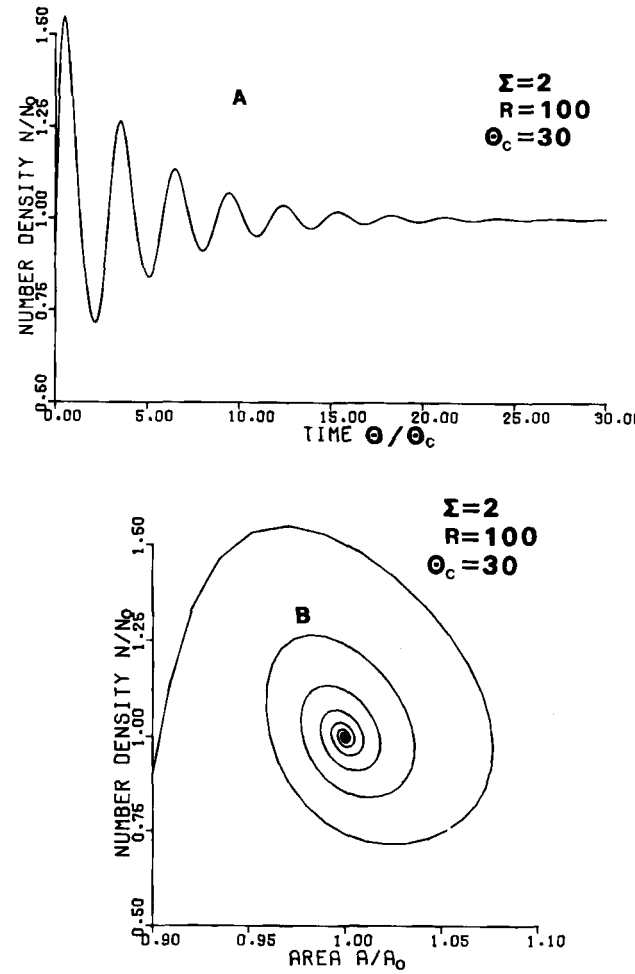

Figure 4. System response in the stable parameter region.
(a) Normalized number density, N/N_0, as a function of normalized time, θ/θ_c. Initial values of S, A, M, and N are 90% of the steady state values, so that the system reaches its steady state after some transient period.
(b) The corresponding phase plot in terms of normalized aerosol number density N/N_0, and aerosol surface area A/A_0.

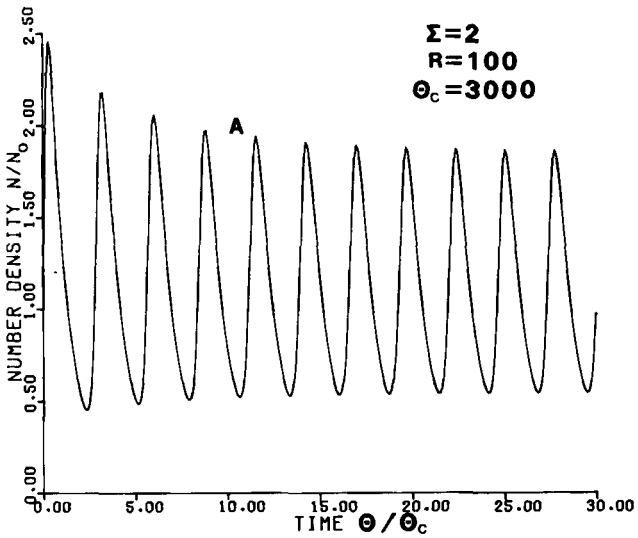

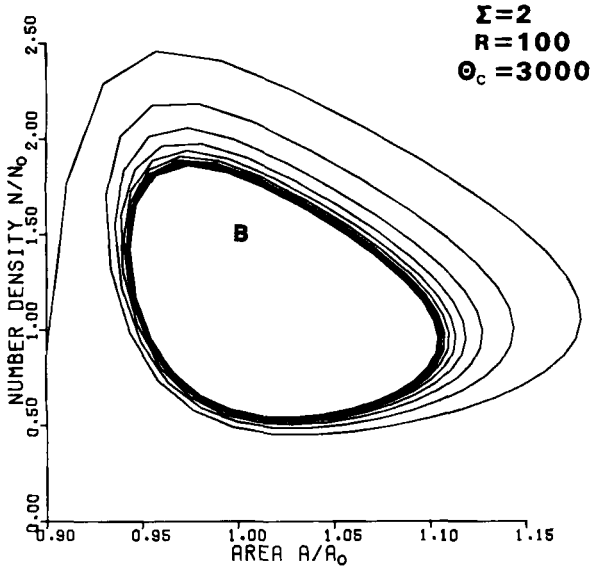

Figure 5. System response in unstable region.

(a) Initial values of *S, A, M,* and *N* are 90% of the steady state values. Dependent variables of the system (here number density is shown) oscillate around their stationary values.

(b) The corresponding phase plot. A limit cycle surrounds the stationary point, (1,1); it is independent of the initial conditions.

ing the oscillations. Figure 7 indicates that both the oscillation amplitude and the average of the maximum and minimum amplitudes of the (presumably periodic) oscillations decrease as θ_c increases. Similar data representation has been done in the classic CSTR stability analysis of Uppal et al. (1974). At this point, we note that numerical integration shows the form of the oscillation (amplitude and period of the stable limit cycle) to be independent of the magnitude of the initial perturbation. For a given combination of θ_c, R, and Σ, there appears to be only one attracting solution.

COMPARISON WITH EXPERIMENTAL RESULTS

Badger and Dryden (1939, Table II) reported the period of observed oscillations and the corresponding values of NO concentration and reactor residence time. Data taken for fixed values of NO

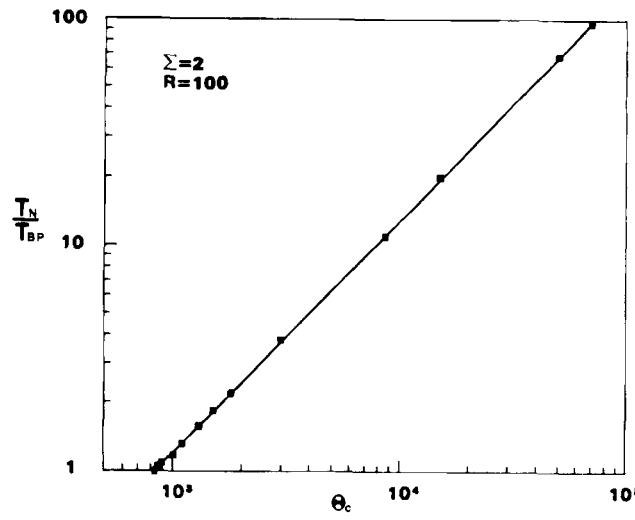

Figure 6. Period of oscillation (T_N) of number density as a function of bifurcation parameter θ_c. Dot corresponds to bifurcation point (*BP*). Here $\theta_{c,BP}$ = 829 and T_{BP} = 2,123.

concentration can be compared with theory through Eq. 21. For constant values of R and Σ, Eq. 21 relates the period of the observed oscillations, T_N, to the residence time of the CSTAR: $T_N = \text{const}\,\tau^h$. Our analysis indicates that $h = 1$ (Figure 6). The experiments of Badger and Dryden for [NO] = 1 ppm and $\tau = 0.65$ h and $\tau = 0.94$ h result in $h = 1.12$.

To compare the form of the oscillations of N given by our model with the observations of Badger and Dryden, Eqs. 7–10 were integrated for arbitrary parameter values (because of the lack of data for R and Σ) in both the stable and unstable regions of the parameter space. The initial conditions were taken as $S_i = 1$, $A_i = M_{1i} = N_i = 0$, where the aerosol moments have been set equal to zero (inlet gas stream was free of particles) as in the experiments of Badger and Dryden. In both the stable and unstable cases, N grows rapidly to an initial maximum, but the longtime behavior is different in the two cases. In the stable part of the pa-

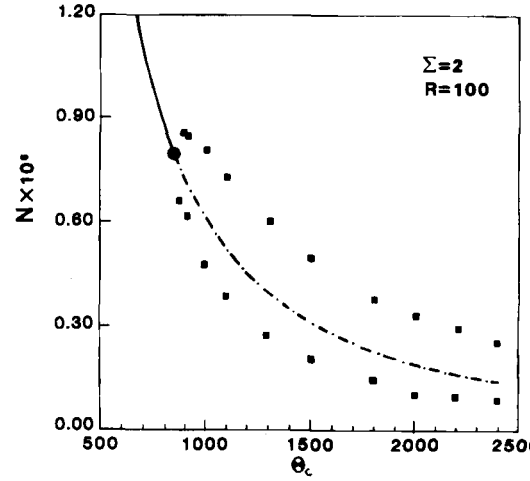

Figure 7. Response diagram of number density *N*, as a function of bifurcation parameter θ_c.

——— Stable operation

–•–•–•– Unstable steady state

■ ■ ■ ■ Envelope of N oscillation in unstable region

● Bifurcation point

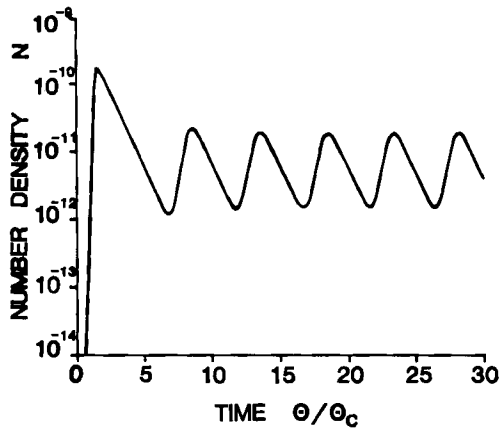

Figure 8. Sample calculation of N as a function of time θ in a CSTAR operating in the unstable region: $\Sigma = 4$, $R = 1$, $\theta_c = 300$. Initial values are $S_i = 1$ and $A_i = M_{1i} = N_i = 0$. Initially N grows rapidly but gradually decreases and after 5–10 residence times exhibits sustained oscillatory behavior.

rameter space, N decreases slowly due to the dilution effect of the flow process, and asymptotically approaches its steady state value. In the unstable region (Figure 8), N gradually decreases as in the stable region, but instead of approaching a steady state value, oscillates about the unstable steady state with an amplitude that varies by an order of magnitude. The shape of the oscillations is related to the physical processes occuring in the system. Thus, one can see that N sharply increases (corresponding to particle formation), and later decreases rather slowly (corresponding to particle removal by the flow process). Similar trends in the behavior of the particle concentration can be seen in Figure 3b of Badger and Dryden (1939). These investigators attributed the rise in N (during the course of the oscillations) to gum vapor condensation on existing ions. Our model provides an alternative explanation of the observed phenomenon by attributing the appearance of successive particle batches to particle formation by homogeneous nucleation.

Badger and Dryden studied the equilibrium between the rate of ion production and the rate of particle removal by outflow. They postulated that oscillations in N appeared for low values of the ratio of NO concentration to reactor residence time, while the reactor exhibited stable behavior for high values of this ratio. Our theory provides a universal criterion (stability map) for the appearance of oscillations in CSTAR's operating under the assumptions stated earlier.

ACKNOWLEDGMENT

This work was supported in part by the National Science Foundation, Grant CPE-81-17288 and a research grant from the Ford Motor Company. S. E. Pratsinis is an Alexander Onassis Fellow.

NOTATION

A	=	aerosol surface area
d_1	=	monomer diameter, m/molecule
$f(S_o)$	=	function of steady state, S_0
I	=	nucleation rate, particles/m$^3 \cdot s$
K	=	mapped interval defined by Eq. 19
k^*	=	critical particle size, molecules/particle
k_B	=	Boltzmann constant
M_1	=	aerosol first moment
m_1	=	monomer mass, kg/molecule
N	=	aerosol number density
n_1	=	monomer concentration, molecules/m^3
n_s	=	monomer concentration at saturation, molecules/m^3
R	=	reaction rate, molecules/m$^3 \cdot s$
S	=	saturation ratio
s_1	=	monomer surface area, m^2/molecule
T	=	temperature, K
T_N	=	dimensionless period of oscillation
T_{BP}	=	dimensionless period of oscillation at the bifurcation point
t	=	time, s
v_1	=	monomer volume, m^3/molecule
$Y^{(v)}$	=	inverse of the midpoint of the interval $[df([S_o^{(v)}])/dS_o]$
$y^{(v)}$	=	midpoint of interval $[S_o^{(v)}]$

Greek Letters

$\alpha,\beta,\gamma,\delta$	=	coefficients of the characteristic equation
θ	=	dimensionless time
θ_c	=	dimensionless residence time
λ	=	complex eigenvalue
λ_{im}	=	imaginary part of λ
λ_r	=	real part of λ
Σ	=	dimensionless surface tension group
σ	=	surface tension, N/m
τ	=	residence time, s

Superscripts

$'$	=	deviation from steady state
v	=	vth interval
overbar	=	upper limit of an interval
underbar	=	lower limit of an interval
$\sim$	=	dimensional

Subscripts

o	=	steady state
i	=	initial value

APPENDIX: COEFFICIENTS OF THE QUARTIC CHARACTERISTIC EQUATION

The characteristic equation is given here by:

$$\begin{vmatrix} -\left(\frac{dIk^*}{dS}\right)_o - \frac{1}{\theta_c} - A_o - \lambda & (S_o - 1) & 0 & 0 \\ \left(\frac{dIk^{*2/3}}{dS}\right)_o + \frac{2}{3}M_{1o} & -\frac{1}{\theta_c} - \lambda & \frac{2}{3}(S_o - 1) & 0 \\ \left(\frac{dIk^{*1/3}}{dS}\right)_o + \frac{1}{3}N_o & 0 & -\frac{1}{\theta_c} - \lambda & \frac{1}{3}(S_o - 1) \\ \left(\frac{dI}{dS}\right)_o & 0 & 0 & -\frac{1}{\theta_c} - \lambda \end{vmatrix} = 0$$

The coefficients of the characteristic equation are obtained after algebraic manipulation of the above equation:

$$\alpha = \left(\frac{dIk^*}{dS}\right)_o + A_o + \frac{4}{\theta_c}$$

$$\beta = \left[\left(\frac{dIk^*}{dS}\right)_o + A_o + \frac{2}{\theta_c}\right]\frac{3}{\theta_c} + (S_o - 1)\left[\left(\frac{dIk^{*2/3}}{dS}\right)_o + \frac{2}{3}M_{1o}\right]$$

$$\gamma = \left[\left(\frac{dIk^*}{dS}\right)_o + A_o + \frac{4}{3\theta_c}\right]\frac{3}{\theta_c^2} + \frac{2(S_o - 1)}{\theta_c}\left[\left(\frac{dIk^{*2/3}}{dS}\right)_o + \frac{2}{3}M_{1o}\right] + \frac{2(S_o - 1)^2}{3}\left[\left(\frac{dIk^{*1/3}}{dS}\right)_o + \frac{1}{3}N_o\right]$$

$$\delta = \left[\left(\frac{dIk^*}{dS}\right)_o + A_o + \frac{1}{\theta_c}\right]\frac{1}{\theta_c^3} + \frac{(S_o - 1)}{\theta_c^2}\left[\left(\frac{dIk^{*2/3}}{dS}\right)_o + \frac{2}{3}M_{1o}\right] + \frac{2(S_o - 1)^2}{3\theta_c}\left[\left(\frac{dIk^{*1/3}}{dS}\right)_o + \frac{1}{3}N_o\right] + \frac{2(S_o - 1)^3}{9}\left(\frac{dI}{dS}\right)_o$$

The roots λ_k of the characteristic equation are the eigenvalues of the linearized system, the solution of which is given by (Denn, 1975):

$$\xi(t) = \sum_j C_k e^{\lambda_k t}$$

LITERATURE CITED

Aris, R., *The Mathematical Theory of Diffusion and Reaction in Permeable Catalysts*, Oxford University Press, II, 80–82, (1975).

Badger, E. H. M., and I. G. C. Dryden, "The Formation of Gum Particles in Coal Gas," *Trans. Faraday Soc.*, 35, 607 (1939).

Becker, C., and H. Reiss, "Nucleation in a Nonuniform Vapor," *J. Chem. Phys.*, 65, 2,066 (1976).

Crump, J. G., and J. H. Seinfeld, "Aerosol Behavior in the Continuous Stirred Tank Reactor," *AIChE J.*, 26, 610 (1980)

Denn, M. M., *Stability of Reaction and Transport Processes*, Prentice-Hall, Englewood Cliffs, NJ, 38 (1975).

Frenkel, J., *Kinetic Theory of Liquids*, Dover, New York, 390–399 (1955).

Friedlander, S. K., *Smoke, Dust and Haze*, Wiley, New York (1977).

———, "The Behavior of Constant Rate Aerosol Reactors," *Aerosol Sci. and Tech.*, 1, 3 (1982).

———, "Dynamics of Aerosol Formation by Chemical Reaction," *Annals NY Acad. Sci.*, 404, 354 (1983).

Heist, R. H., A. Fuchs, and G. Agarwal, "Multiple Oscillations at High Rates of Homogeneous Nucleation," *Chem. Eng. Com.*, 5, 1 (1980).

Henry, J. F., A. Gonzalez, and L. K. Peters, "Dynamics of NH_4Cl Particle Nucleation and Growth at 253–296 K," *Aerosol Sci. and Tech.*, 2, 321 (1983).

IMSL, *IMSL Contents Document*, 8th ed., Int. Math. and Statistical Libraries, Houston (1980).

Jerauld, G. R., Y. Vasatis, and M. F. Doherty, "Simple Conditions for the Appearance of Sustained Oscillations in Continuous Crystallizers," *Chem. Eng. Sci.*, 38, 1,675 (1983).

Karman, T., and M. A. Biot, *Mathematical Methods in Engineering*, McGraw-Hill, New York, 244 (1940).

Krawczyk, R., "Newton Algorithms for the Determination of Zeros with Error Limits," *Computing*, 4, 187 (1969)

Lee, J. C.-M., "Stability of Distributed Chemical Reaction Systems," Ph.D. Diss., Univ. of Houston (1970).

Marsden, J. E., and M. McCracken, *The Hopf Bifurcation and Its Applications*, Springer-Verlag, New York, 163–205 (1976).

Moore, R. E., and S. T. Jones, "Safe Starting Regions for Iterative Methods," *SIAM J. Numerical Anal.*, 14, 611 (1977).

Moore, R. E., "Methods and Applications of Interval Analysis," *SIAM Studies in Appl. Math.*, Philadelphia, 9–15, (1979).

Randolph, A. D., "CSD Dynamics, Stability and Control", *AIChE Symp. Ser.* 76, 1 (1980).

Reiss, H., D. C. Marvin, and R. H. Heist, "The Use of Nucleation and Growth as a Tool in Chemical Physics," *J. Colloid Interface Sci.*, 58, 125 (1977).

Sherwin, M. B., R. Shinnar, and S. Katz, "Dynamic Behavior of the Well-Mixed Isothermal Crystallizer," *AIChE J.*, 13, 1,141 (1967).

Uppal, A., W. H. Ray, and A. B. Poore, "On the Dynamic Behavior of Continuous Stirred Tank Reactors," *Chem. Eng. Sci.*, 29, 967 (1974).

Manuscript received June 12, 1984, and revision received Mar. 14, 1985.